Morphological Analysis of Disabled-1-Immunoreactive Amacrine Cells in the Guinea Pig Retina

EUN-JIN LEE,[1] HYUN-JU KIM,[1] IN-BEOM KIM,[1] JAE-HYUNG PARK,[1] SU-JA OH,[1] DENNIS W. RICKMAN,[2,3] AND MYUNG-HOON CHUN[1]*
[1]Department of Anatomy, College of Medicine, The Catholic University of Korea, Seoul 137-701, Korea
[2]Department of Ophthalmology, Duke University, Durham, North Carolina 27710
[3]Department of Neurobiology, Duke University, Durham, North Carolina 27710

ABSTRACT

Disabled-1 (Dab1) is an adapter molecule in a signaling pathway, stimulated by *reelin*, that controls cell positioning in the developing brain. It localizes to selected neurons in the nervous system, including the retina, and Dab1-like immunoreactivity is present in AII amacrine cells in the mouse retina. This study was conducted to characterize Dab1-labeled cells in the guinea pig retina in detail using immunocytochemistry, quantitative analysis, and electron microscopy. Dab1 immunoreactivity is present in a class of amacrine cell bodies located in the inner nuclear layer adjacent to the inner plexiform layer (IPL). These cells give rise to processes that ramify the entire depth of the IPL. Double-labeling experiments demonstrated that these amacrine cells make contacts with the axon terminals of rod bipolar cells and that their processes make contacts with each other via connexin 36 in sublamina b of the IPL. In addition, all Dab1-labeled amacrine cells showed glycine transporter 1 immunoreactivity, indicating that they are glycinergic. The density of Dab1-labeled AII amacrine cells decreased from about 3,750 cells/mm^2 in the central retina to 1,725 cells/mm^2 in the peripheral retina. Dab1-labeled amacrine cells receive synaptic inputs from the axon terminals of rod bipolar cells in stratum 5 of the IPL. From these morphological features, Dab1-labeled cells of the guinea pig retina resemble the AII amacrine cells described in other mammalian species. Thus, the rod pathway of the guinea pig retina follows the general mammalian scheme and Dab1 antisera can be used to identify AII amacrine cells in the mammalian retina. J. Comp. Neurol. 466:240–250, 2003.

Indexing terms: connexin 36; glycine transporter-1; AII amacrine cells; rod bipolar cells; immunocytochemistry

Disabled 1 (Dab1) is a cytoplasmic protein that is expressed and tyrosine-phosphorylated in the developing mammalian nervous system (Howell et al., 1997). It also functions as an adapter molecule in a signaling pathway, stimulated by *Reelin*, that regulates the final positioning of neurons (Rice and Curran, 1999). Rice and Curran (2000) have demonstrated that Dab1 is expressed in mouse retinal cells that exhibit features of type AII amacrine cells, important interneurons in the rod pathway of the mammalian retina. Such AII amacrine cells are located in the proximal inner nuclear layer (INL) adjacent to the inner plexiform layer (IPL). They are distinctly bistratified cells with a thick primary process and distinct arborizations—so-called lobular appendages—in sublamina a, and bushy dendritic fields in sublamina b of the IPL (Famiglietti and Kolb, 1975; Vaney, 1985; Dacheux and Raviola, 1986; Wong et al., 1986; Young and Vaney, 1990; Mills and Massey, 1991; Vaney et al., 1991; Strettoi et al., 1992; Wässle et al., 1993, 1995; Rice and Curran,

Grant sponsor: the Korea Science and Engineering Foundation; Grant number: F01-2000-000-10021-0; Grant sponsor: the National Institutes of Health; Grant number: EY 11389.

*Correspondence to: Myung-Hoon Chun, Department of Anatomy, College of Medicine, The Catholic University of Korea, 505 Banpo-dong, Sochogu, Seoul 137-701, Korea. E-mail: mhchun@catholic.ac.kr

Received 5 March 2003; Revised 6 May 2003; Accepted 13 June 2003
DOI 10.1002/cne.10870
Published online the week of September 22, 2003 in Wiley InterScience (www.interscience.wiley.com).

2000). This cell type represents the major output of rod bipolar cells and feeds their signals into the cone pathway by making conventional inhibitory chemical (putative glycinergic) synapses with OFF-cone bipolar cells and OFF-ganglion cells in sublamina a. They also make electrical synapses (through gap junctions) with ON-cone bipolar cells in sublamina b of the IPL (Kolb and Famiglietti, 1974; Famiglietti and Kolb, 1975, 1979; Pourcho, 1982; McGuire et al., 1984; Dacheux and Raviola, 1986; Raviola and Dacheux, 1987; Voigt and Wässle, 1987; Sterling et al., 1988; Kolb et al., 1990; 1991; Strettoi et al., 1990, 1992; Chun et al., 1993). AII amacrine cells are themselves interconnected by gap junctions at their dendrites in the IPL (Kolb and Famiglietti, 1974). In the nervous system, a number of different connexins are expressed in astrocytes and oligodendrocytes (Dermietzel and Spray, 1998), in pigment epithelial cells, as well as in photoreceptor cells in the vertebrate retina (O'Brien et al., 1996; Janssen-Bienhold et al., 2001). Recently, Cx36 protein has been located in membrane contacts between both types of coupled neighboring cells of AII amacrine cells in mouse, rat, and rabbit retinas (Feigenspan et al., 2001; Guldenagel et al., 2001; Mills et al., 2001). Coupling between the AII amacrine cells is believed to improve the signal-to-noise ratio at low light levels, whereas coupling between AII amacrine cells and cone bipolar cell may facilitate the transition from rod to cone vision (Vaney, 1994; Mills and Massey, 1995).

The morphology and topographic distributions of retinal AII amacrine cells have been described in the cat (Vaney, 1985), rabbit (Mills and Massey, 1991; Vaney et al., 1991), rat (Wässle et al., 1993), and mouse (Rice and Curran, 2000). AII amacrine cells are numerous, with a higher cell density in the central retina than in the peripheral retina. They constitute about 10% of all retinal amacrine cells in the rat, cat, and rabbit (Vaney, 1985; Mills and Massey, 1991; Vaney et al., 1991; Wässle et al., 1993). However, AII amacrine cells have not been described in the guinea pig retina, which has relatively more cones than rat and mouse retinas. We therefore investigated this in detail using immunocytochemistry, quantitative analysis, and electron microscopy to clarify whether the rod pathway might have common features across mammalian species.

MATERIALS AND METHODS

Tissue preparation

Five adult guinea pigs of either sex were used and two mice were used as controls. The animals were treated according to the regulations of the Catholic Ethics Committee of the Catholic University of Korea, Seoul, which conforms to all National Institutes of Health (NIH) guidelines. The animals were killed by an intraperitoneal overdose (4 ml/100 g body weight) of 4% chloral hydrate and the eyes were enucleated. The anterior segments were removed and the eyecups were fixed by immersion in 4% paraformaldehyde in 0.1 M phosphate buffer (PB), pH 7.4, for 2–3 hours. Following fixation, the retinas were carefully dissected and transferred to 30% sucrose in PB for 24 hours at 4°C. They were then frozen in liquid nitrogen, thawed, and rinsed in 0.01 M phosphate-buffered saline (PBS, pH 7.4).

Immunocytochemistry

Immunostaining was performed using indirect immunofluorescence or the avidin–biotin–peroxidase complex (ABC) method (Hsu et al., 1981). Whole-mount preparations and 50-μm thick vibratome sections were incubated in 10% normal goat serum (NGS) and 1% Triton X-100 in PBS for 1 hour at room temperature to block nonspecific binding sites. The sections were then incubated with a rabbit polyclonal antibody directed against Dab1 (kindly provided by Dr. B. Howell, NIH) and used at a dilution of 1:1,000 for immunostaining in PBS containing 0.5% Triton X-100 for 3 days at 4°C. Retinas were washed in PBS for 45 minutes (3 × 15 min), incubated for 12 hours in Cy3-conjugated antirabbit IgG (1:100: Jackson ImmunoLabs, West Grove, PA) or biotinylated goat antirabbit IgG (Vector Laboratories, Burlingame, CA) with 0.5% Triton X-100 at 4°C and rinsed in PBS. For the ABC method, they were subsequently incubated in ABC solution (Vector Laboratories) in PBS for 12 hours at 4°C. Retinas were rinsed in two changes of PBS and three changes of 0.05 M Tris-HCl buffer (TB), pH 7.6, for 5 minutes each at room temperature, then incubated in 0.05% 3,3′-diaminobenzidine tetrahydrochloride (DAB) in TB for 10 minutes. For whole-mount immunostaining, the same immunocytochemical procedures described above were used, but with longer incubation times. Hydrogen peroxide was added to the incubation medium to a final concentration of 0.01%. The container was gently shaken as the reaction proceeded. The reaction was stopped with several washes of TB and PB after 1–2 min, as determined by the degree of staining. The retinas were mounted on gelatin-coated slides with the ganglion cell layer (GCL) facing upward and coverslips were applied with glycerol. For light microscope analysis, 50-μm thick vibratome sections were photographed using an Olympus microscope (Olympus Co., Japan). The micrographs in Figure 1 were taken on 35 mm monochrome film (Kodak; plus-X pan, 125 ASA) using differential interference contrast optics (Japan).

For double-labeling studies, sections were incubated overnight in a mixture of anti-Dab1 antibody (1:1,000) with the following antibodies and dilutions: mouse monoclonal anti-GAD_{65} (Chemicon, Temecula, CA; diluted to 1:500); monoclonal anti-Cx35/36 (Chemicon; 1:1,000); monoclonal anti-protein kinase C (PKC: Sigma, St. Louis, MO; 1:500); monoclonal anti-calretinin (Chemicon; 1:10,000), and goat polyclonal anti-glycine transporter 1 antibody (Chemicon; 1:10,000), all with 0.5% Triton X-100 in 0.1 M PBS at 4°C.

Sections were rinsed for 30 minutes with 0.1 M PBS and incubated in fluorescein isothiocyanate (FITC)-conjugated affinity-purified antimouse IgG and antigoat IgG (1:100: Jackson) and Cy3-conjugated antirabbit IgG (1:100: Jackson) for 1–2 hours at room temperature. Sections were washed for 30 minutes with 0.1 M PB and coverslipped with 10% glycerol in 0.1 M PB containing 2% KI. To ensure that the secondary antibody had not cross-reacted with the inappropriate primary antibody, some sections were incubated in rabbit and goat polyclonal primary antibodies followed by antimouse secondary antibody, and other sections were incubated in mouse primary antibody followed by antirabbit secondary antibody. These sections did not show any immunostaining.

Confocal laser scanning microscopy

Sections were analyzed using a Bio-Rad Radiance Plus confocal scanning microscope (Bio-Rad, Hemel Hempstead, UK), installed on a Nikon Eclipse E600 fluorescence microscope (Nikon, Tokyo, Japan). FITC and Cy3 signals were always detected separately. FITC labeling was excited using the 488 nm line of an argon ion laser and detected after passing a HQ513/30 (Bio-Rad) emission filter. For detection of the Cy3 signal, the 543-nm line of the green HeNe laser was used in combination with the 605/32 (Bio-Rad) emission filter. Images were imported into Adobe PhotoShop v. 5.5 (Mountain View, CA) and photographed onto slide film (Kodak Ektachrome 100; Eastman Kodak, Rochester, NY). For presentation, all manipulations (brightness and contrast only) were carried out equally.

Electron microscopy

Three adult guinea pigs were euthanized as described above. The eyecups were fixed in a mixture of 4% paraformaldehyde and 0.2% picric acid in PB for 30 minutes at room temperature. The retinas were then carefully dissected; small pieces were taken from the central region and fixed for an additional 2 hours at 4°C. After being washed in PB, the retinal pieces were transferred to 30% sucrose in PB for 6 hours at 4°C, rapidly frozen in liquid nitrogen, thawed, and embedded in 4% agar in distilled water. The retinal pieces were sectioned using a vibratome at 50 μm and the sections were placed in PBS. They were incubated in 10% NGS in PBS for 1 hour at room temperature to block nonspecific binding and were then incubated in Dab1 antibody diluted 1:1,000 for 12 hours at 4°C.

The following immunocytochemical procedures were carried out at room temperature. The sections were washed in PBS for 45 minutes (3 × 15), incubated in biotin-labeled goat antirabbit IgG for 2 hours, then washed three times in PBS for 45 minutes (3 × 15). The sections were incubated in ABC solution for 1 hour, washed in TB, then incubated in 0.05% DAB solution containing 0.01% H_2O_2. The reaction was monitored using a low-power microscope and was stopped by replacing the DAB and H_2O_2 solution with TB.

The stained sections were postfixed in 1% glutaraldehyde in PB for 1 hour. After being washed in PB containing 4.5% sucrose for 15 minutes (3 × 5), they were postfixed in 1% OsO_4 in PB for 1 hour. They were washed again in PB containing 4.5% sucrose and dehydrated in a graded series of alcohol. During the dehydration procedure they were stained en bloc with 1% uranyl acetate in 70% alcohol for 1 hour, infiltrated in propylene oxide, and flat-embedded in Epon 812. After the sections had been cured at 60°C for 3 days, well-stained areas were cut out and attached to an Epon support for further ultrathin sectioning using a Reichert-Jung ultratome. Ultrathin sections (70–90 nm thick) were collected on one-hole grids coated with Formvar and examined using a transmission electron microscope (JEOL model 1200EX, Tokyo, Japan).

Topography and quantitation

The topography and quantitation of the Dab1-immunoreactive cell populations were analyzed in two well-stained retinas. The data for the density maps were plotted using conventional microscopy. For the density maps, a field of 200 × 200 μm^2 was sampled in 1-mm steps of the retina from superior to inferior. Nearest-neighbor analysis (Wässle and Riemann, 1978) was performed on the cells located in mid-peripheral regions of the retina. The results were not corrected for shrinkage of the tissue during the mounting process, as this was negligible.

RESULTS

To test the specificity of the Dab1 antibody, two sets of controls were run. In the first, mouse retina was used. In the second set, normal rabbit serum (preimmune serum) was applied to the sections of the guinea pig retina. In Figure 1A, amacrine cells with lobular appendages and narrow dendritic fields are visible in the mouse retina, as described by Rice and Curran (2000). No immunostaining in the guinea pig retina was seen in the section immunostained with preimmune serum (Fig. 1B).

Dab1 immunoreactivity in the guinea pig retina

Dab1 immunoreactivity was observed in a single, morphologically distinct population of amacrine cells with somata located in the proximal row of the INL. No immunoreactivity was observed in the outer nuclear layer, the outer plexiform layer, or the ganglion cell layer.

Vertical sections of guinea pig retina immunolabeled for Dab1 are shown in Figure 2. The somata of Dab1 immunoreactive cells were strongly immunostained and found in the INL adjacent to the IPL border (Fig. 2). These amacrine cells typically have a single primary dendrite that descends into the IPL and then gives off several side branches, which run towards strata 5 near the ganglion cell layer. In sublamina a, thin and short immunoreactive processes with large, irregular endings originated from the primary process. These processes resembled the lobular appendages previously described for AII amacrine cells of the rabbit, cat, rat, and mouse retinas (Famiglietti and Kolb, 1975; Vaney, 1985; Dacheux and Raviola, 1986; Wong et al., 1986; Mills and Massey, 1991; Young and Vaney, 1990; Vaney et al., 1991; Strettoi et al., 1992; Wässle et al., 1993, 1995; Rice and Curran, 2000).

In whole-mount retinal preparations, when we focused on the INL numerous Dab1-immunoreactive amacrine cell somata were distributed throughout the retina (Fig. 3A). These were round or pyriform in shape. In Figure 3B, taken at a higher magnification than Figure 3A, the lobules are clearly visible in sublamina a of the IPL. Figure 3C, taken from the same retinal field as Figure 3B at a different focal plane within the inner aspect of the IPL, shows a few processes ramifying in stratum 5 of the IPL. The terminal branches of labeled cells were difficult to trace, as they intermingled with other labeled processes originating from other Dab1-labeled cells.

Double immunofluorescence for Dab1 with protein kinase C and Connexin 36

The AII amacrine cell is one of two types of postsynaptic amacrine cells at rod bipolar ribbon synapses (Kolb and Famiglietti, 1974; Famiglietti and Kolb, 1975; Kolb, 1979; Pourcho, 1982; McGuire et al., 1984; Dacheux and Raviola, 1986; Raviola and Dacheux, 1987; Voigt and Wässle, 1987; Sterling et al., 1988; Kolb et al., 1990, 1991; Strettoi et al., 1990, 1992; Chun et al., 1993; Wässle et al.,

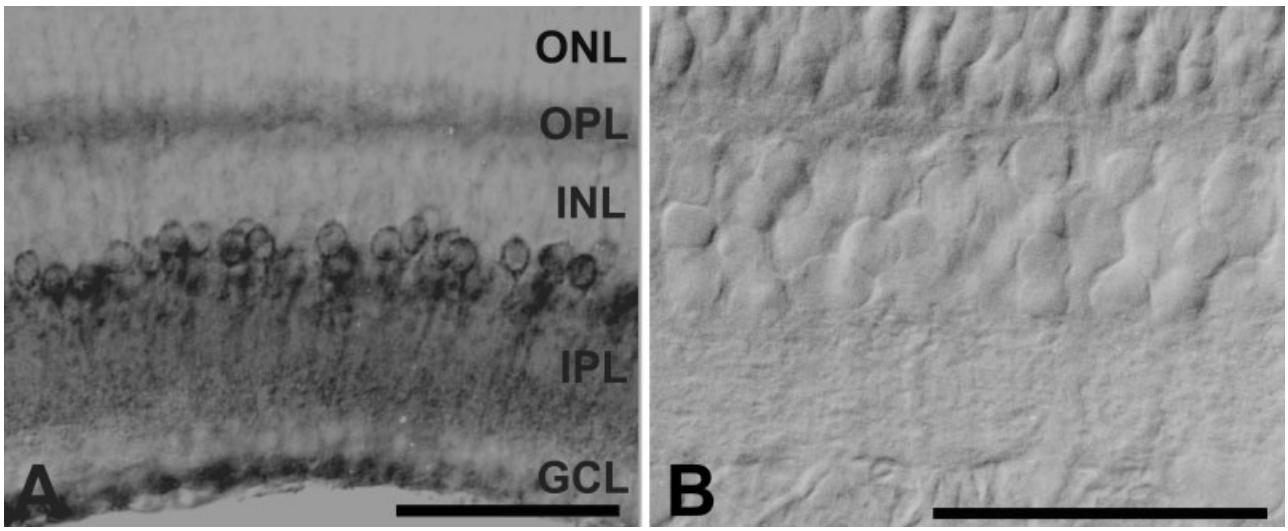

Fig. 1. Light micrographs taken from 50-μm thick vertical vibratome sections of the mouse retina (**A**) processed for Dab1 immunoreactivity and the guinea pig retina (**B**) immunostained with preimmune serum. A: Amacrine cells with lobular appendages and narrow dendritic fields are visible. B: No immunostaining is seen. ONL, outer nuclear layer; OPL, outer plexiform layer; INL, inner nuclear layer; IPL, inner plexiform layer; GCL, ganglion cell layer. Scale bar = 50 μm.

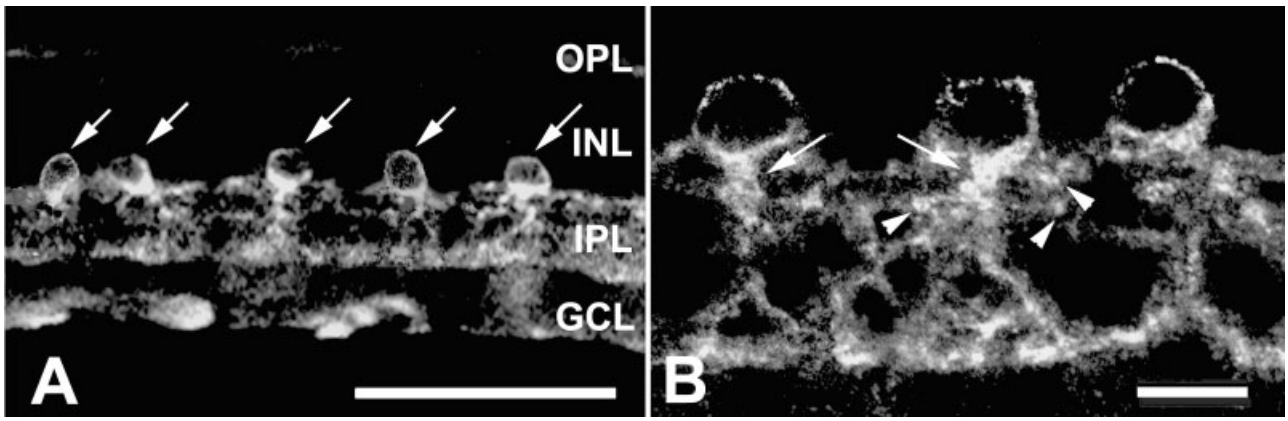

Fig. 2. Light micrographs taken from 50-μm thick vertical vibratome sections processed for Dab1 immunoreactivity. **A:** Dab1 immunoreactivity is present in amacrine cell bodies (arrows) located in the proximal INL and in processes located in the entire length of the IPL. **B:** A single primary dendrite (arrows) emerging from a cell body and lobular appendages (arrowheads) are visible in sublamina a of the IPL. In sublamina b, labeled processes form a diffuse network of dendrites. Scale bars = 50 μm in A; 10 μm in B.

1995). Protein kinase C (PKC) is primarily expressed by rod bipolar cells in the mammalian retina (Negishi et al., 1988; Greferath et al., 1990), and was therefore used to identify rod bipolar cells in the guinea pig retina. Figure 4A–C shows vertical sections of the guinea pig retina double-labeled with antibodies against Dab1 (Fig. 4A) and PKC (Fig. 4B). PKC-immunoreactivity was found in the cell bodies and in their axons, which terminated close to the ganglion cell layer. Figure 4C shows rod bipolar axon terminal systems that appear to be decorated or attached to the surface with AII amacrine cell processes. We also examined whether Cx36 protein immunoreactivity was associated with the fine dendritic processes of neighboring AII amacrine cells. We double-labeled Dab1 (Fig. 4D) and Cx36 (Fig. 4E); this demonstrated weak labeling in sublamina a, whereas strong puncta labeling was detected throughout sublamina b of the IPL. Double-labeling with Cx36 antibody clearly indicated that Cx36 is localized adjacent to the dendrites of AII amacrine cells (Fig. 4F). Such a close localization appeared to be mostly restricted to sublamina b of the IPL, whereas cell bodies and lobular appendages in sublamina a did not show significant overlap of Cx36 and Dab1 immunostaining (Fig. 4F).

Dab1-labeled amacrine cells show GlyT-1 immunoreactivity

In the mammalian retina, most amacrine cells contain either glycine or γ-aminobutyric acid (GABA) (Marc, 1989; Vaney, 1990; Marc et al., 1995; Vardi and Auerbach, 1995). In addition, the Dab1-labeled cells appear to be morphologically reminiscent of AII amacrine cells in the mammalian retina (Vaney et al., 1991; Wässle et al., 1993;

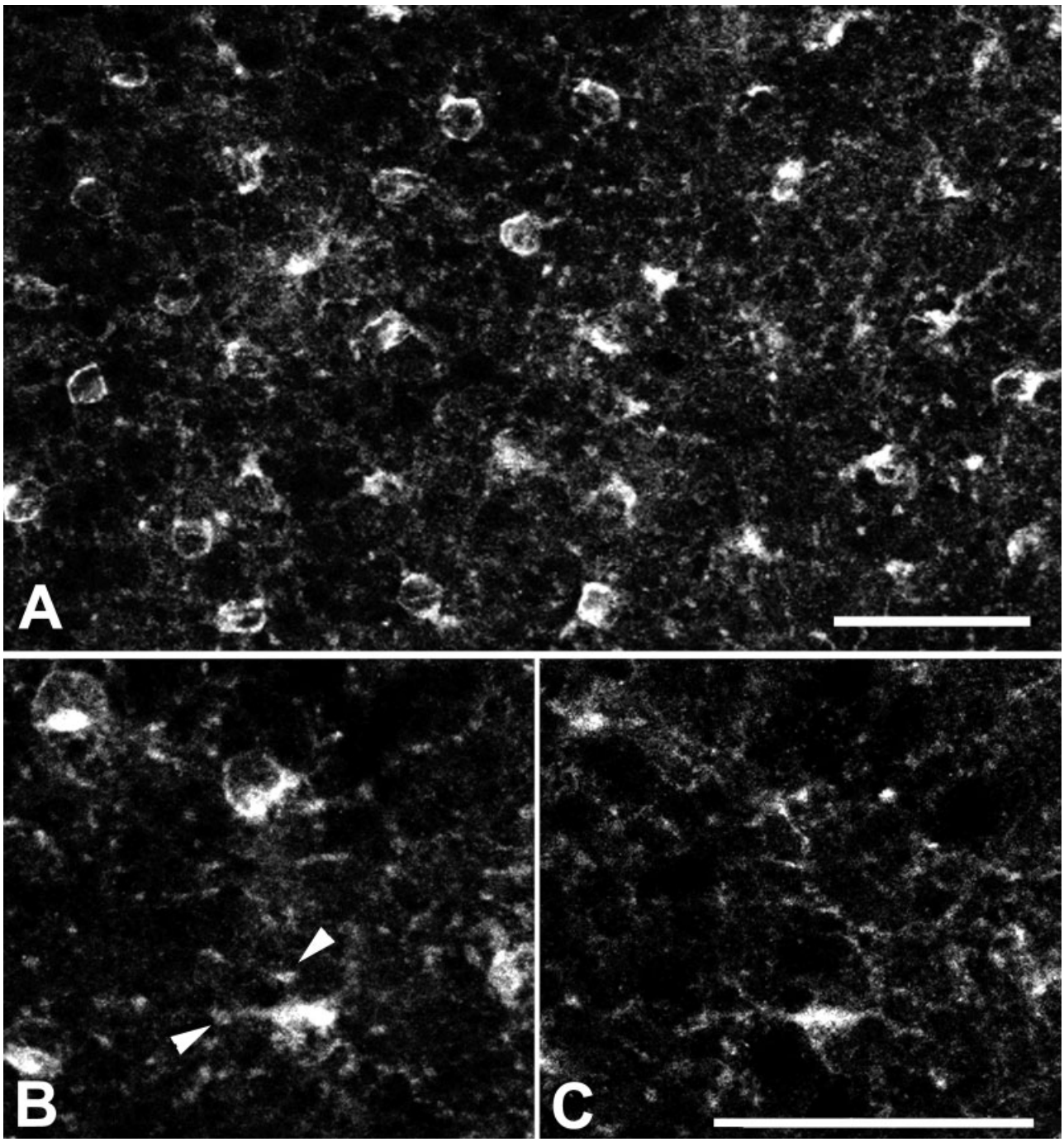

Fig. 3. Light micrographs taken at different focal planes in the same field of a whole-mount guinea pig retina processed for Dab1 immunoreactivity. **A:** Low-power micrograph focused at the Dab1-labeled amacrine cell bodies. The numerous small dots are lobular appendages. **B,C:** Higher-power microphotographs taken from the same field at different focal planes. B: The focus is on the IPL close to the INL. The labeled cell bodies are out of focus and lobular appendages (arrowheads) are seen. C: The focus is on the IPL close to the GCL. Bushy processes of Dab1-labeled amacrine cells are visible. Scale bars = 50 μm.

Strettoi et al., 1994; Massey and Mills, 1999; Mills and Massey, 1999; Rice and Curran, 2000; Bloomfield, 2001), which are glycinergic (Grünert and Wässle, 1993; Menger et al., 1998; Rice and Curran, 2000). Thus, we further characterized the Dab1-labeled amacrine cells neurochemically to determine whether Dab1-labeled amacrine cells are glycinergic or GABAergic. We performed double-labeling using antisera against Dab1 and either glycine transporter 1 (Glyt-1) or GAD_{65}. Figure 4G–L shows vibratome sections that were double-labeled with antibodies

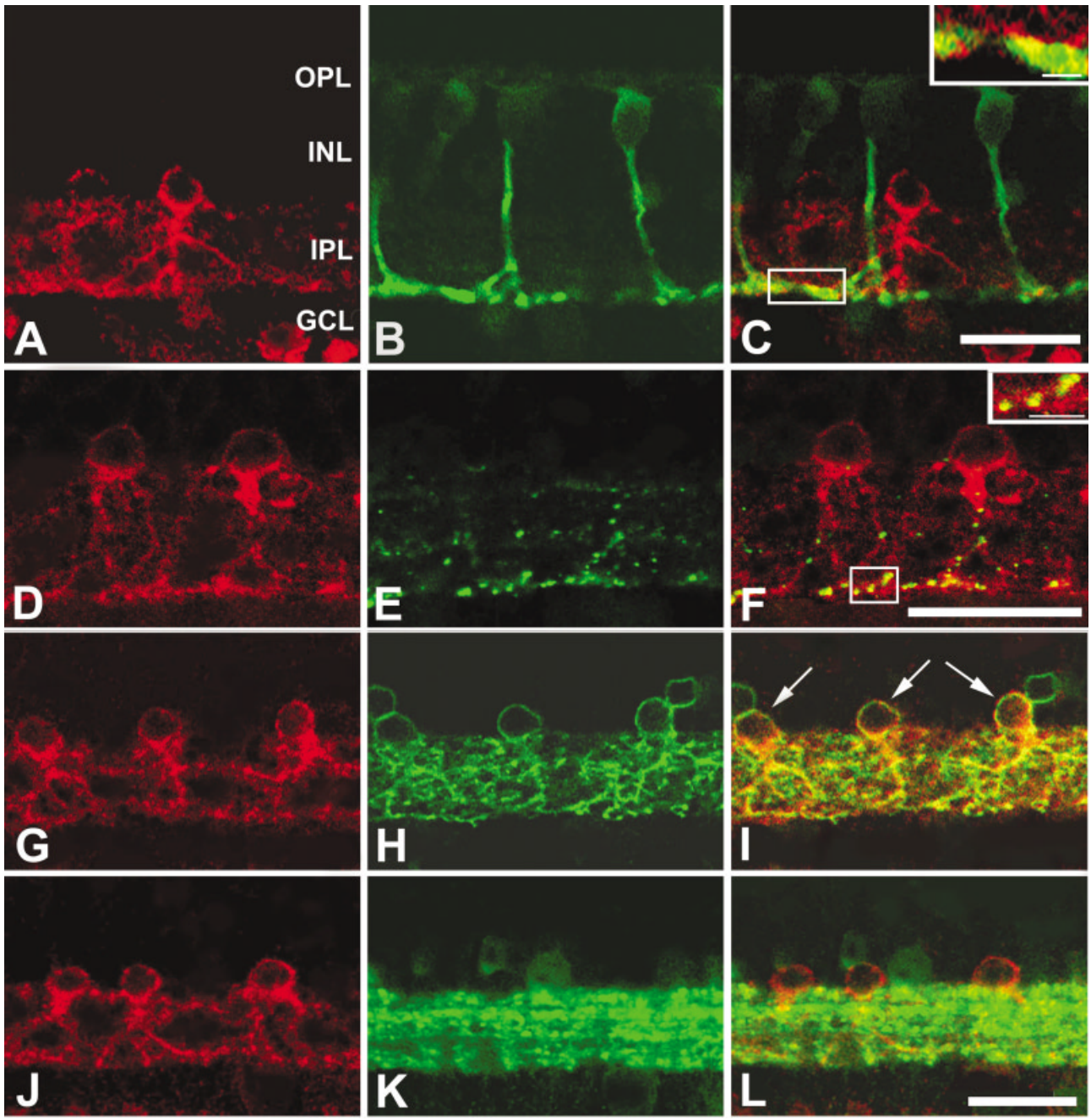

Fig. 4. Confocal micrographs taken from 50-μm thick vertical vibratome sections processed for Dab1 (**A,D,G,J**) and PKC (**B**), Cx35/36 (**E**), Glyt-1 (**H**), or GAD65 (**K**) immunoreactivities. Dab1 immunoreactivity was visualized using a Cy3-conjugated secondary antibody. Protein kinase C (PKC), Cx35/36, GlyT-1, and GAD65 immunoreactivities were visualized using an FITC-conjugated secondary antibody. A,D: Two Dab1 immunoreactive cell bodies are visible. B: PKC immunoreactive cell bodies and terminals are visible. **C:** Double exposure of A and B shows that Dab1 processes are localized adjacent to the rod bipolar terminals (yellow). The inset rectangle shows a high-magnification view. E: Cx35/36 immunoreactivity appears as discrete puncta, densely in the sublamina b and sparsely in the sublamina a of the IPL. **F:** Double exposure of D and E. Colocalization (yellow) of Cx35/36 and Dab1 immunoreactivities is visible in sublamina b of the IPL. G, J: Three Dab1-labeled cell bodies (red) are seen. H: Five Glyt-1 immunoreactive cell bodies (green) are visible in the INL. **I:** Double exposure of G and H. Colocalization (yellow) of DAB1 and GlyT-1 within the same cell (arrows) is clear. K: Several GAD_{65} immunoreactive cell bodies are visible in the INL. **L:** Double exposure of D and E shows that no colocalization of Dab1 and GAD65 immunoreactivities are visible. The inset rectangle shows a high-magnification view. Scale bars = 30 μm; 5 μm in insets.

against Dab1 (Fig. 4G,J) and Glyt-1 (4H) or GAD_{65} (4K). As observed in the merged confocal image of a vertical section in Figure 4I, three Dab1-labeled amacrine cells also showed Glyt-1 immunoreactivity. All Dab1-labeled amacrine cells examined in this study (n = 57) showed Glyt-1 immunoreactivity; thus, the Dab1-labeled ama-

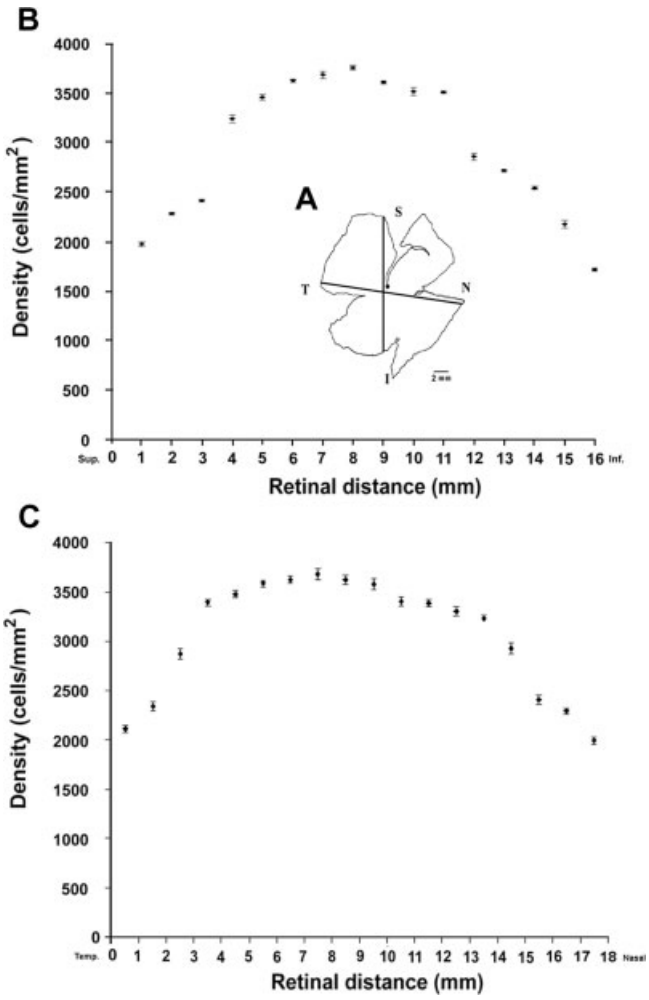

Fig. 5. Density of Dab1-immunoreactive cells in a whole mount of a guinea pig retina. The black line in the map of the whole mount indicates the intersection along which the density measurements were taken. **A:** A map of the whole mount. **B:** From superior region to inferior region. **C:** Temporal region to nasal region. S, superior; T, temporal; I, inferior; N, nasal. Scale bar = 2 μm.

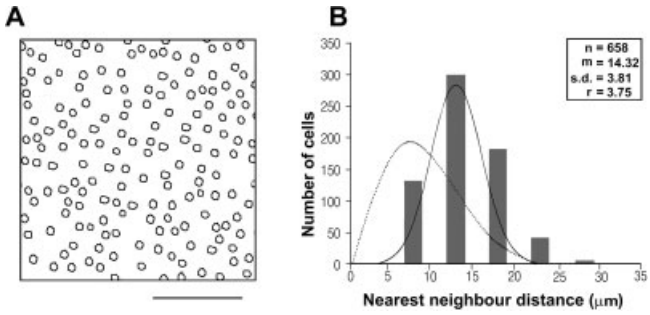

Fig. 6. Nearest-neighbor analysis of the Dab1 immunoreactive amacrine cells in the inner nuclear layer. Left: Drawings of part of the analyzed field in the mid-peripheral regions of the retina; Dab1 immunoreactive amacrine cells appear rather regularly spaced. Right: Nearest-neighbor distance histograms for Dab1 immunoreactive amacrine cells (hatched) in the mid-peripheral region. Each histogram for Dab1 immunoreactive amacrine cells are relatively well matched by a Gaussian curve (solid line), which describes a regular cell distribution, but not by a Poisson curve (dotted line), which describes a random cell distribution (Rayleigh distribution). Each histogram shows the number of cells in the sample (n), the mean distance between cells (m), the standard deviation (s.d.), and regularity index (r). Scale bar = 100 μm.

crine cells constitute a subpopulation of glycinergic amacrine cells. However, there was no colocalization of Dab1 and GAD_{65} immunoreactivities within the same amacrine cells, as is evident from the merged Figure 5L.

Quantitative analysis

The quantitative studies characterized the Dab1-immunoreactive amacrine cell population. The density of Dab1-immunoreactive amacrine cells was measured from superior to inferior retina or from nasal to temporal retina of a whole mount (Fig. 5). The Dab1-labeled AII amacrine cell density peaked at 3,750 ± 11.2 cells/mm^2 in the central region around the optic disc; it was 2,700 ± 12.2 cells/mm^2 elsewhere and was least at the retinal periphery, with 1,725 ± 10.0 cells/mm^2.

To assess the distribution of Dab1-immunoreactive amacrine cell quantitatively, we used nearest-neighbor analysis (Wässle and Riemann, 1978). The distance of each soma to its nearest neighbor was measured in 0.25 × 0.25 mm areas of the mid-peripheral retina. The resulting histogram for the mid-peripheral retinal region is shown in Figure 6 (right). The histogram fits a Gaussian distribution fairly well in terms of mean distances and standard deviations (solid lines), indicating a statistically regular mosaic of labeled cells in this region, but do not fit a Poisson curve (dotted line), which describes a random cell distribution (Rayleigh distribution)

Electron microscopy of Dab1-labeled cells

Dab1 immunoreactivity produced an electron-dense reaction product that was closely associated with mitochondrial membranes, cytoplasmic matrices, and synaptic vesicles. Figure 7 shows an example of a rod bipolar axon terminal making a ribbon synapse. One labeled amacrine (AII) process (here with a large mitochondrion) and one unlabeled amacrine cell process comprise the postsynaptic dyad. These AII amacrine cells are almost invariably postsynaptic to rod bipolar cells (Kolb and Famiglietti, 1974; Famiglietti and Kolb, 1975; Kolb, 1979; Pourcho, 1982; McGuire et al., 1984; Dacheux and Raviola, 1986; Raviola and Dacheux, 1987; Voigt and Wässle, 1987; Sterling et al., 1988; Kolb et al., 1990, 1991; Strettoi et al., 1990, 1992; Chun et al., 1993; Wässle et al., 1995), so the presence of labeling in one of the postsynaptic processes again confirms that the Dab1 antibody is a good selective marker for such cells. However, one process is unlabeled and makes a reciprocal synapse onto the rod bipolar axon. This may be an example of GABAergic amacrine cells, which have been shown to make reciprocal synapses with rod bipolar terminals (Chun and Wässle, 1989; Strettoi et al., 1990; Kim et al., 1998).

Double immunofluorescence for Dab1 and AII amacrine cell marker

A few immunocytochemical markers that recognize AII amacrine cells, such as antisera against parvalbumin (Wässle et al., 1995), calretinin (Wässle et al., 1995; Mas-

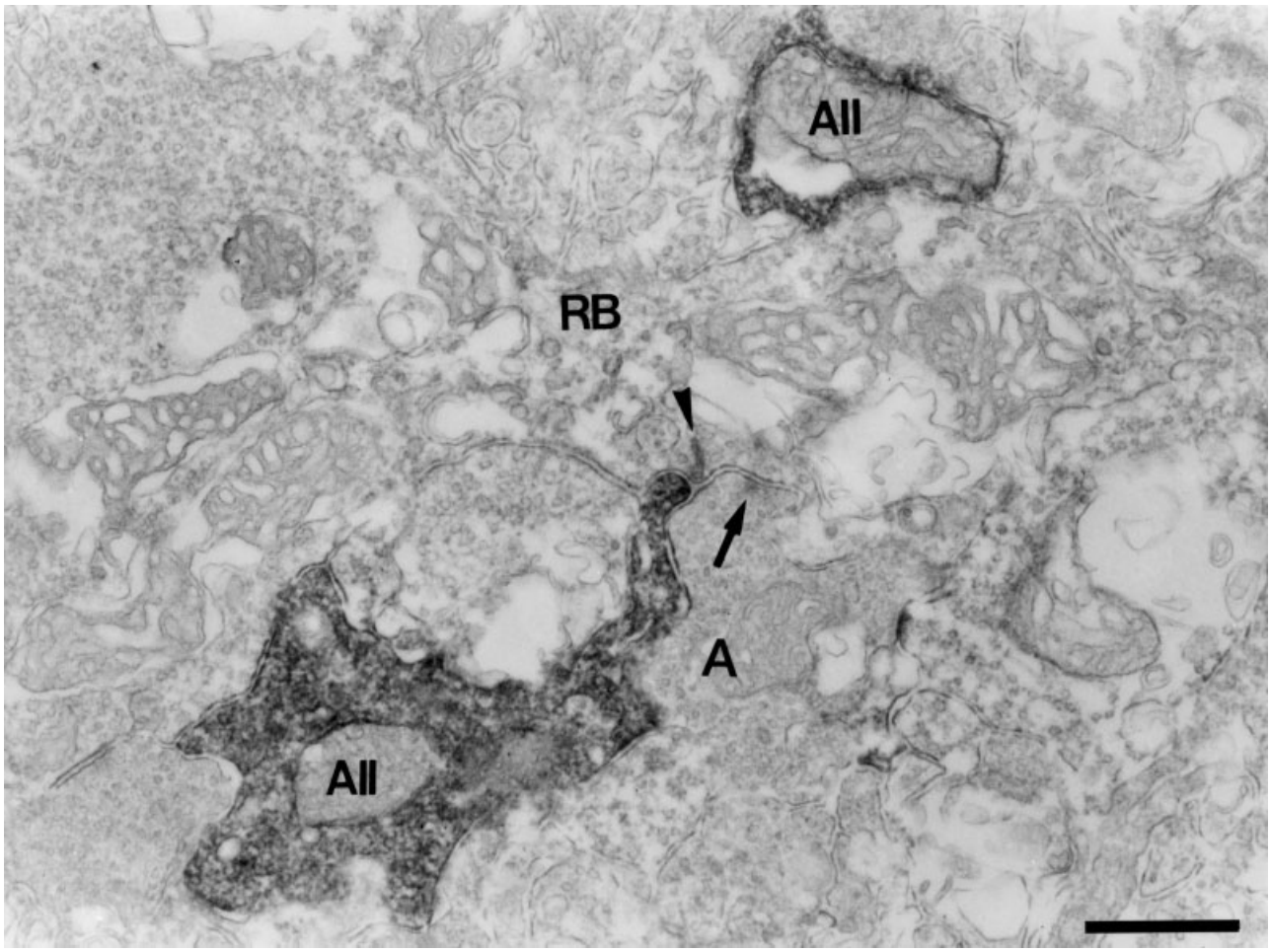

Fig. 7. Electron micrograph taken from a vertical ultrathin section in stratum 5 of the IPL of the guinea pig retina processed for Dab1 immunoreactivity. A Dab1-labeled amacrine cell process (AII) with a large mitochondrion comprises a postsynaptic dyad with another unlabeled amacrine cell process (A) at the ribbon synapse of a rod bipolar terminal (RB). The unlabeled amacrine cell process in turn makes a chemical synapse (arrow) onto the rod bipolar terminal. Arrowhead indicates a synaptic ribbon. Scale bar = 0.5 μm.

sey and Mills, 1999; Mills and Massey, 1999), and Dab1 (Rice and Curan, 2000), have been applied to the retina of cat, rabbit, primate, rat, and mouse. To identify whether Dab1 and calretinin or parvalbumin immunoreactivities are expressed within the same amacrine cells, double-labeling experiments were performed. Figure 8 shows an example of vibratome sections double-labeled with antisera against Dab1 and calretinin. Figure 8A was processed for Dab1 immunoreactivity and Figure 8B was processed for calretinin immunoreactivity. In a merged figure (Fig. 8C), there is colocalization of Dab1 and calretinin immunoreactivities within amacrine cells located in the proximal row of the INL. Dab1 immunoreactivity was observed in all calretinin-immunoreactive amacrine cells examined in this study (n = 63), but such cells did not show parvalbumin immunoreactivity (data not shown).

DISCUSSION

This study characterized the morphology, distribution, neurochemical properties, and synaptic connectivity of Dab1-immunoreactive neurons in the guinea pig retina, using light and electron microscopic immunocytochemistry. Dab1 immunoreactivity has been studied in the mouse retina, where Rice and Curran (2000) showed that it is first detectable after birth, and that it persists primarily in type AII amacrine cells, which are the main interneurons in the rod pathway. Here, we found that the morphology of Dab1-immunoreactive amacrine cells of the guinea pig retina is in agreement with earlier investigations showing that AII amacrine cells also express parvalbumin or calretinin immunoreactivity (Endo et al., 1985, 1986; Röhrenbeck et al., 1987, 1989; Celio, 1990; Sanna et al., 1990, 1993; Gabriel and Straznicky, 1992; Wässle et al., 1993; reviewed in MacNeil et al., 1999). Dab1 immunoreactivity was present in a single row of the cells in the proximal INL and in the thick primary processes that descend and ramify in sublaminae a and b of the IPL. In addition, the immunoreactive cells are round or pyriform in shape and have large swellings (lobular appendages) that arise from their descending processes in the IPL (Famiglietti and Kolb, 1975; Vaney, 1985; Dacheux and Raviola, 1986; Wong et al., 1986; Mills and Massey, 1991;

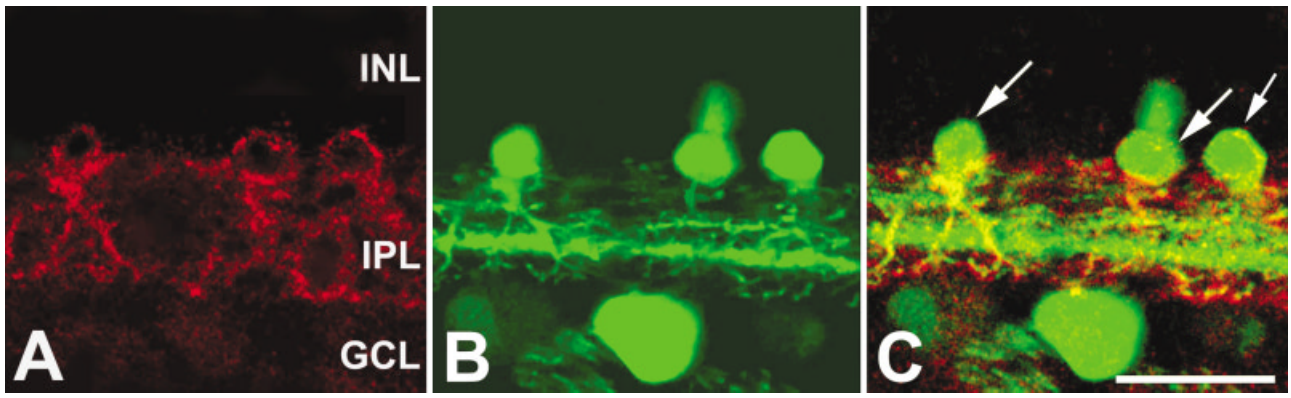

Fig. 8. Confocal micrographs taken from a 50-μm thick vertical vibratome section processed for Dab1 (**A**) and calretinin (**B**) immunoreactivities. Dab1 immunoreactivity was visualized using a Cy3-conjugated secondary antibody. Calretinin immunoreactivity was visualized using an FITC-conjugated secondary antibody. A: Three Dab1 immunoreactive cell bodies are seen. B: Four calretinin-labeled amacrine cell in the INL bodies and one labeled large cell body in the GCL are visible. **C:** Double exposure of A and B. Colocalization (yellow) of Dab and calretinin within the same amacrine cell bodies located in the proximal row of the INL (arrows) is clear. Scale bar = 30 μm.

Young and Vaney, 1990; Vaney et al., 1991; Strettoi et al., 1992; Wässle et al., 1993, 1995; Rice and Curran, 2000).

In the retina, the neuron-specific protein Cx36 is expressed in AII amacrine cells and might comprise a subunit of AII–AII connections (Feigenspan et al., 2001; Mills et al., 2001). Punctate labeling of Cx36 in sublamina a of the guinea pig IPL did not overlap significantly with the lobular appendages of AII amacrine cells; this is in agreement with a report that showed lack of gap junctions in this region (Strettoi et al., 1992). Hence, in the guinea pig retina, Cx36 immunoreactivity present in sublamina a might belong to other cell types present in the INL or GCL. Cx36 in the guinea pig retina may also form homotypic gap junctional channels with neighboring AII amacrine cells within stratum 5 of the IPL, similar to that seen in the rabbit retina (Strettoi et al., 1992) and forms heterotypic gap junctional channels with ON bipolar cells in sublamina b (Strettoi et al., 1992). This electrotonic pathway is believed to transmit the rod signal to the cone ON pathway (Vaney, 1997).

The Dab1-immunoreactive amacrine cells in the guinea pig retina were further characterized by double-label immunocytochemistry using a marker for glycinergic amacrine cell populations. Amacrine cells exist in two major groups: glycinergic and GABAergic amacrine cells (Vaney, 1990). Glycinergic amacrine cells are well characterized as small-field cells with branching dendrites (Pourcho and Goebel, 1985; Menger et al., 1998). Here, all the Dab1-immunoreactive amacrine cells contained GlyT-1 immunoreactivity, demonstrating that they are functionally glycinergic (Zafra et al., 1995; Vaney et al., 1998). This result is in agreement with studies in the rat and mouse retina showing that AII cells express Glyt-1 (Menger et al., 1998; Rice and Curran, 2000).

We found that the Dab1-immunoreactive cell density was highest in the central retina with about 3,750 cells/mm^2, and lowest in the peripheral retina with about 1,725 cells/mm^2, in accord with previous reports on the rabbit (Casini et al., 1995) and mouse retina (Rice and Curran, 2000). In addition, the Dab1-labeled amacrine cells form a nonrandom mosaic, as shown by the distribution of their nearest-neighbor distances. The regularity of a cell mosaic is expressed by the regularity index, which is the ratio between the mean of the nearest-neighbor distances and its standard deviation. A ratio of 1.0 indicates a random distribution and the higher this ratio, the more regular the distribution (Eberhardt, 1967; Wässle and Riemann, 1978). In this study, the regularity index was 3.75, which is in good agreement with that of the AII amacrine cell mosaic in the rabbit retina stained by parvalbumin antibody (Mills and Massey, 1991; Vaney et al., 1991). This suggests that the putative AII-type cells form a homogenous population.

We used electron microscopy to study the synaptic relationships between rod bipolar cells and Dab1-labeled amacrine cells in stratum 5 of the IPL. At the rod bipolar dyad, one of the postsynaptic elements is a narrow-field amacrine cell type (Kolb and Famiglietti, 1974; Famiglietti and Kolb, 1975; Kolb, 1979; Pourcho, 1982; McGuire et al., 1984; Dacheux and Raviola, 1986; Raviola and Dacheux, 1987; Voigt and Wässle, 1987; Sterling et al., 1988; Kolb et al., 1990, 1991; Strettoi et al., 1990, 1992; Chun et al., 1993; Wässle et al., 1995), which contains glycine as an inhibitory transmitter (Frederick et al., 1984; Pourcho and Goebel, 1985, 1987; Hendrickson et al., 1988; Crooks and Kolb, 1992; Koonz et al., 1993). The other is an indoleamine-accumulating (Sandell et al., 1989), putative GABAergic (Osborne and Beaton, 1986; Lim et al., 1998), depolarizing amacrine cell type that corresponds to the A17 type in the cat (Nelson and Kolb, 1985; Raviola and Dacheux, 1987). As expected from the immunofluorescence findings, these glycinergic Dab1-labeled amacrine cell processes comprised postsynaptic dyads with other unlabeled amacrine cell processes at ribbon synapses of the rod bipolar cells, as shown in other mammalian retinas (Kolb and Famiglietti, 1974; Famiglietti and Kolb, 1975; Kolb, 1979; Pourcho, 1982; McGuire et al., 1984; Dacheux and Raviola, 1986; Raviola and Dacheux, 1987; Voigt and Wässle, 1987; Sterling et al., 1988; Kolb et al., 1990, 1991; Strettoi et al., 1990, 1992; Chun et al., 1993; Wässle et al., 1995).

Dab1-labeled amacrine cells have been further confirmed using AII amacrine cell markers in other species using antibodies against calcium-binding proteins: calretinin in primates (Wässle et al., 1995; Massey and Mills, 1999; Mills and Massey, 1999); parvalbumin in the cat, rat, and rabbit (Gabriel and Straznicky, 1992; Wässle et al., 1993; Casini et al., 1995); and Dab1 in the mouse (Rice and Curran, 2000). In the present study, all Dab1-immunoreactive cells showed calretinin but not parvalbumin immunoreactivity. This is not surprising, as the distribution of some markers in the vertebrate retina tends to vary phylogenetically (Marc, 1986; Mandell et al., 1990). We conclude that Dab1 and calretinin—but not parvalbumin—can be used to label AII amacrine cells in the guinea pig retina.

In conclusion, Dab1 immunoreactivity in the guinea pig retina is localized to a population of bi-stratified amacrine cells that are identical to the AII amacrine cells described in other mammals. Thus, based on their morphology, distribution, and neurochemical content, there is strong evidence that the Dab1-immunoreactive amacrine cells in the proximal INL of the guinea pig retina are indeed AII amacrine cells. Dab1 is therefore a reliable marker for the visualization of AII amacrine cell population in the guinea pig retina. This approach to immunostaining will facilitate more general characterization and understanding of the rod pathway in the mammalian retina.

LITERATURE CITED

Bloomfield SA. 2001. Plasticity of AII amacrine cell circuitry in the mammalian retina. Prog Brain Res 131:185–200.

Casini G, Rickman DW, Brecha NC. 1995. AII amacrine cell population in the rabbit retina: identification by parvalbumin immunoreactivity. J Comp Neurol 356:132–142.

Celio MR. 1990. Calbindin D-28k and parvalbumin in the rat nervous system. Neuroscience 35:375–475.

Chun MH, Wässle H. 1989. GABA-like immunoreactivity in the cat retina: electron microscopy. J Comp Neurol 279:55–67.

Chun MH, Han SH, Chung JW, Wässle H. 1993. Electron microscopic analysis of the rod pathway of the rat retina. J Comp Neurol 332:421–432.

Crooks J, Kolb H. 1992. Localization of GABA, glycine, glutamate and tyrosine hydroxylase in the human retina. J Comp Neurol 315:287–302.

Dacheux RF, Raviola E. 1986. The rod pathway in the rabbit retina: a depolarizing bipolar and amacrine cell. J Neurosci 6:331–345.

Dermietzel R. Spray DC. 1998. From neuro-glue ('Nervenkitt') to glia: a prologue. Glia 24:1–7.

Eberhardt LL. 1967. Some developments in 'distance sampling.' Biometrics 23:207–216.

Endo T, Kobayashi S, Onaya T. 1985. Parvalbumin in rat cerebrum, cerebellum and retina during postnatal development. Neurosci Lett 60:279–282.

Endo T, Kobayashi M, Kobayashi S, Onaya T. 1986. Immunocytochemical and biochemical localization of parvalbumin in the retina. Cell Tissue Res 243:213–217.

Famiglietti EV, Kolb H. 1975. A bistratified amacrine cell and synaptic circuitry in the inner plexiform layer of the retina. Brain Res 84:293–300.

Feigenspan A, Teubner B, Willecke K, Weiler R. 2001. Expression of neuronal connexin36 in AII amacrine cells of the mammalian retina. J Neurosci 21:230–239.

Frederick JM, Rayborn ME, Hollyfield JG. 1984. Glycinergic neurons in the human retina. J Comp Neurol 227:159–172.

Gabriel R, Straznicky C. 1992. Immunocytochemical localization of parvalbumin- and neurofilament triplet protein immunoreactivity in the cat retina: colocalization in a subpopulation of AII amacrine cells. Brain Res 595:133–136.

Greferath U, Grünert U, Wässle H. 1990. Rod bipolar cells in the mammalian retina show protein kinase C-like immunoreactivity. J Comp Neurol 301:433–442.

Grünert U, Wässle H. 1993. Immunocytochemical localization of glycine receptors in the mammalian retina. J Comp Neurol 335:523–537.

Guldenagel M, Ammermuller J, Feigenspan A, Teubner B, Degen J, Sohl G, Willecke K, Weiler R. 2001. Visual transmission deficits in mice with targeted disruption of the gap junction Gene connexin36. J Neurosci 21:6036–6044.

Hendrickson AE, Koontz MA, Pourcho RG, Sarthy PV, Goebel DJ. 1988. Localization of glycine-containing neurons in the Macaca monkey retina. J Comp Neurol 273:473–487.

Howell BW, Hawkes R, Soriano P, Cooper JA. 1997. Neuronal position in the developing brain is regulated by mouse disabled-1. Nature 369: 733–737.

Hsu SM, Raine L, Fanger H. 1981. Use of avidin-biotin-peroxidase complex (ABC) in immunoperoxidase techniques: a comparison between ABC and unlabeled antibody (PAP) procedures. J Histochem Cytochem 29: 577–580.

Janssen-Bienhold U, Schultz K, Gellhaus A, Schmidt P, Ammermuller J, Weiler R. 2001. Identification and localization of connexin26 within the photoreceptor-horizontal cell synaptic complex. Vis Neurosci 18:169–178.

Kim IB, Lee MY, Oh S, Kim KY, Chun M. 1998. Double-labeling techniques demonstrate that rod bipolar cells are under GABAergic control in the inner plexiform layer of the rat retina. Cell Tissue Res 292:17–25.

Kolb H. 1979. The inner plexiform layer in the retina of the cat: electron microscopic observations. J Neurocytol 8:295–329.

Kolb H. 1997. Amacrine cells of the mammalian retina: neurocircuitry and functional roles. Eye 11:904-23.

Kolb H, Famiglietti EV. 1974. Rod and cone pathways in the inner plexiform layer of cat retina. Science 186:47–49.

Kolb H, Cuenca N, Wang HH, Dekorver L. 1990. The synaptic organization of the dopaminergic amacrine cell in the cat retina. J Neurocytol 19:343–66.

Kolb H, Cuenca N, Wang HH, Dekorver L. 1991. Postembedding immunocytochemistry for GABA and glycine reveals the synaptic relationships of the dopaminergic amacrine cell of the cat retina. J Comp Neurol 310:267–284.

Koontz MA, Hendrickson LE, Brace ST, Hendrickson AE. 1993. Immunocytochemical localization of GABA and glycine in amacrine and displaced amacrine cells of macaque monkey retina. Vision Res 33:2617–2628.

Lim CH, Ho SM. 1998. GABAergic modulation of axonal conduction in the developing rat retinotectal pathway. Brain Res Dev Brain Res 108: 299–302.

MacNeil MA, Heussy JK, Dacheux RF, Raviola E, Masland RH. 1999. The shapes and numbers of amacrine cells: matching of photofilled with Golgi-stained cells in the rabbit retina and comparison with other mammalian species. J Comp Neurol 413:305–326.

Mandell JW, Townes-Anderson E, Czernik AJ, Cameron R, Greengard P, De Camilli P. 1990. Synapsins in the vertebrate retina: absence from ribbon synapses and heterogeneous distribution among conventional synapses. Neuron 5:19–33.

Marc RE. 1986. Neurochemical stratification in the inner plexiform layer of the vertebrate retina. Vision Res 26:223–238.

Marc RE. 1989. The role of glycine in the mammalian retina. Prog Ret Res 8:67–107.

Marc RE, Murry RF, Basinger SF. 1995. Pattern recognition of amino acid signatures in retinal neurons. J Neurosci 15:5106–129.

Massey SC, Mills SL. 1999. Antibody to calretinin stains AII amacrine cells in the rabbit retina: double-label and confocal analyses. J Comp Neurol 411:3–18.

McGuire GA, Stevens JK, Sterling P. 1984. Microcircuitry of bipolar cells in cat retina. J Neurosci 4:2920–2938.

Menger N, Pow DV, Wässle H. 1998. Glycinergic amacrine cells of the rat retina. J Comp Neurol 401:34–46.

Mills SL, Massey SC. 1991. Labeling and distribution of AII amacrine cells in the rabbit retina. J Comp Neurol 304:491–501.

Mills SL, Massey SC. 1995. Differential properties of two gap junctional pathways made by AII amacrine cells. Nature 377:676–677.

Mills SL, Massey SC. 1999. AII amacrine cells limit scotopic acuity in central macaque retina: A confocal analysis of calretinin labeling. J Comp Neurol 411:19–34.

Mills SL, O'Brien JJ, Li W, O'Brien J, Massey SC. 2001. Rod pathways in the mammalian retina use connexin 36. J Comp Neurol 436:336–50.

Negishi K, Kato S, Teranishi T. 1988. Dopamine cells and rod bipolar cells contain protein kinase C-like immunoreactivity in some vertebrate retinas. Neurosci Lett 94:247–252.

Nelson R, Kolb H. 1985. A17: a broad-field amacrine cell in the rod system of the cat retina. J Neurophysiol 54:592–614.

O'Brien J, Al-Ubaidi MR, Ripps H. 1996. Connexin35: a gap-junctional protein expressed preferentially in the skate retina. Mol Biol Cell 7:233–243.

Osborne NN, Beaton DW. 1986. The occurrence of gamma-aminobutyric acid (GABA)-containing cells in cultures of retinas from the human fetus. Cell Mol Neurobiol 6:87–93.

Pourcho RG. 1982. Dopaminergic amacrine cells in the cat retina. Brain Res 252:101–109.

Pourcho RG, Goebel DJ. 1985. A combined Golgi and autoradiographic study of (3H)glycine-accumulating amacrine cells in the cat retina. J Comp Neurol. 233:473–480.

Raviola E, Dacheux RF. 1987. Excitatory dyad synapse in rabbit retina. Proc Natl Acad Sci USA 84:7324–7328.

Rice DS, Curran T. 1999. Mutant mice with scrambled brains: understanding the signaling pathways that control cell positioning in the CNS. Genes Dev 13:2758–2773.

Rice DS, Curran T. 2000. Disabled-1 is expressed in type AII amacrine cells in the mouse retina. J Comp Neurol 424:327–338.

Röhrenbeck J, Wässle H, Heizmann CW. 1987. Immunocytochemical labelling of horizontal cells in mammalian retina using antibodies against calcium-binding proteins. Neurosci Lett 77:255–260.

Röhrenbeck J, Wassle H, Boycott BB. 1989. Horizontal cells in the monkey retina: immunocytochemical staining with antibodies against calcium binding proteins. Eur J Neurosci 1:407–420.

Sandell JH, Masland RH, Raviola E, Dacheux RF. 1989. Connections of indoleamine-accumulating cells in the rabbit retina. Comp Neurol 283: 303–313.

Sanna PP, Keyser KT, Battenberg E, Bloom FE. 1990. Parvalbumin immunoreactivity in the rat retina. Neurosci Lett 118:136–139.

Sanna PP, Keyser KT, Celio MR, Karten HJ, Bloom FE. 1993. Distribution of parvalbumin immunoreactivity in the vertebrate retina. Brain Res 600:141–50.

Sterling P. 1983. Microcircuitry of the cat retina. Annu Rev Neurosci 6:149–185.

Sterling P, Freed MA, Smith RG. 1988. Architecture of rod and cone circuits of the on-beta ganglion cell. J Neurosci 8:623–642.

Strettoi E, Dacheux RF. 1992. Synaptic connections of the narrow-field, bistratified rod amacrine cell (AII) in the rabbit retina. J Comp Neurol 325:152–168.

Strettoi E, Dacheux RF, Raviola E. 1990. Synaptic connections of rod bipolar cells in the inner plexiform layer of the rabbit retina. J Comp Neurol 295:449–466.

Strettoi E, Dacheux RF, Raviola E. 1994. Cone bipolar cells as interneurons in the rod pathway of the rabbit retina. J Comp Neurol 347:139–149.

Vaney DI. 1985. The morphology and topographic distribution of AII amacrine cells in the cat retina. Proc R Soc Lond B Biol Sci 224:475–488.

Vaney DI. 1990. The mosaic of amacrine cells in the mammalian retina. Prog Ret Res 9:49–100.

Vaney DI. 1994. Patterns of neuronal coupling in the retina. Prog Ret Eye Res 13:301–355.

Vaney DI. 1997. Neuronal coupling in rod-signal pathways of the retina. Invest Ophthalmol Vis Sci 38:267–273.

Vaney DI, Gynther IC, Young HM. 1991. Rod-signal interneurons in the rabbit retina: 2. AII amacrine cells. J Comp Neurol 310:154–169.

Vaney DI, Nelson JC, Pow DV. 1998. Neurotransmitter coupling through gap junctions in the retina. J Neurosci 18:10594–10602.

Vardi N, Auerbach P. 1995. Specific cell types in cat retina express different forms of glutamic acid decarboxylase. J Comp Neurol 351:374–384.

Voigt T, Wässle H. 1987. Dopaminergic innervation of AII amacrine cells in mammalian retina. J Neurosci 7:4115–4128.

Wässle H, Riemann HJ. 1978. The mosaic of nerve cells in the mammalian retina. Proc R Soc Lond B Biol Sci 200:441–461.

Wässle H, Grünert U, Röhrenbeck J. 1993. Immunocytochemical staining of AII-amacrine cells in the rat retina with antibodies against parvalbumin. J Comp Neurol 332:407–420.

Wässle H, Grünert U, Chun MH, Boycott BB. 1995. The rod pathway of the macaque monkey retina: identification of AII-amacrine cells with antibodies against calretinin. J Comp Neurol 361:537–551.

Wong ROL, Henry GH, Medveczky CJ. 1986. Bistratified amacrine cells in the retina of the Tammar wallaby—*Macropus eugenii*. Exp Brain Res 63:102–105.

Young HM, Vaney DI. 1990. The retinae of prototherian mammals possess neuronal types that are characteristic of non-mammalian retinae. Vis Neurosci 5:61–66.

Zafra F, Aragon C, Olivares L, Danbolt NC, Gimenez C, Storm-Mathisen J. 1995. Glycine transporters are differentially expressed among CNS cells. J Neurosci 15:3952–3969.